

NUMERICAL STUDY OF FRACTIONAL CAMASSA-HOLM EQUATIONS

CHRISTIAN KLEIN* AND GOKSU ORUC

ABSTRACT. A numerical study of fractional Camassa-Holm equations is presented. Smooth solitary waves are constructed numerically. Their stability is studied as well as the long time behavior of solutions for general localised initial data from the Schwartz class of rapidly decreasing functions. The appearance of dispersive shock waves is explored.

1. INTRODUCTION

This paper is concerned with the numerical study of solutions to the fractional Camassa-Holm (fCH) equation given by

$$(1) \quad u_t + \kappa_1 u_x + 3uu_x + D^\alpha u_t = -\kappa_2 [2D^\alpha(uu_x) + uD^\alpha u_x],$$

where κ_1, κ_2 are real constants. The fractional derivative D^α (also called fractional Laplacian) is defined via its Fourier symbol

$$(2) \quad \mathcal{F}D^\alpha = |k|^\alpha,$$

where \mathcal{F} denotes the Fourier transform and where k is the dual Fourier variable, see (6).

1.1. **Background.** In the case $\alpha = 2$, $\kappa_1 = 2\omega$ and $\kappa_2 = \frac{1}{3}$, the equation (1) turns into the Camassa Holm (CH) equation

$$(3) \quad u_t + 2\omega u_x + 3uu_x - u_{xxt} = 2u_x u_{xx} + uu_{xxx}.$$

The CH equation was first introduced in [21] in a formal study of a class of integrable equations. In [4] the CH equation was presented to model unidirectional propagation of small-amplitude shallow water waves above a flat bottom. It has been also derived as geodesic flow on the circle in [10, 11, 32] and recently in the context of nonlinear dispersive elastic waves in [16]. The CH equation is completely integrable and has an infinite number of local conserved quantities [20], three of which are given in the following form:

$$H_0 = \int_{\mathbb{R}} u dx, \quad H_1 = \frac{1}{2} \int_{\mathbb{R}} (u^2 + u_x^2) dx, \quad H_2 = \frac{1}{2} \int_{\mathbb{R}} (u^3 + uu_x^2 + 2\omega u^2) dx.$$

The CH equation has smooth solitary wave solutions and peaked solitons (*peakons*) in the cases $\omega > 0$ and $\omega = 0$, respectively. The existence of peaked solitary waves has been established in [2]. A classification of travelling wave solutions that also contain cusped solitons (*cuspons*) has been proposed in [35]. The orbital stability of the travelling waves has been obtained for smooth solitons in [13], for peakons in [12] and for periodic peakons in [33, 34]. Wave breaking phenomena which cause solutions to remain bounded whereas their slopes blow up in finite time have

Date: September 27, 2023.

This work was partially supported by the ANR-17-EURE-0002 EIPHI, the Bourgogne Franche-Comté Region, the European fund FEDER, and by the European Union Horizon 2020 research and innovation program under the Marie Skłodowska-Curie RISE 2017 grant agreement no. 778010 IPaDEGAN. .

been investigated in [9]. Many numerical approaches for the CH equation have been developed such as finite difference methods, finite-volume methods, pseudo-spectral methods, local discontinuous Galerkin methods, see for instance [25, 7, 8, 3, 27, 40, 19, 5, 23, 1].

Even though the CH equation has been studied extensively, there are only few results on the fractional CH equation which has been obtained in [16] via a multi-scales expansion for a fractional Boussinesq equation appearing in elasticity. In [15] the local well-posedness of the Cauchy problem to the following form of fractional CH equation

$$(4) \quad u_t + u_x + \frac{1}{2}(u^2)_x + \frac{3}{4}D^\alpha u_x + \frac{5}{4}D^\alpha u_t = -\frac{1}{4}[2D^\alpha(uu_x) + uD^\alpha u_x]$$

has been proven for the initial data $u_0 \in H^s(\mathbb{R})$, $s > \frac{5}{2}$ when $\alpha > 2$ via Kato's semigroup approach for quasilinear evolution equations. In [18] the local well-posedness criteria for the same Cauchy problem has been refined in an appropriate Besov space as $B_{2,1}^{s_0}$ with $s_0 = 2\alpha - \frac{1}{2}$ for $\alpha > 3$ and $s_0 = \frac{5}{2}$ for $2 < \alpha \leq 3$. In [17] the local well-posedness results given in [18] have been recently extended to the Cauchy problem for the generalized fractional CH equation

$$(5) \quad u_t + u_x + \frac{1}{2}(u^{p+1})_x + \frac{3}{4}D^\alpha u_x + \frac{5}{4}D^\alpha u_t = -\frac{p+1}{8}[2D^\alpha(u^p u_x) + u^p D^\alpha u_x]$$

with $\alpha > 2$ and $p \in \mathbb{N}^+$. A blow-up criterion for the solutions has been obtained. We note here that in the standard case ($\alpha = 2$) the equation (4) is related to well known integrable shallow water equation derived in [14]. To the best of our knowledge there is no study related to fractional CH equation when $\alpha \leq 2$ and the current paper is the first numerical study on the fractional CH equation in the literature.

1.2. Main results. In this paper we always consider positive values of the constant $\kappa_1 = 2\omega$. For the CH equation it is known that the solitary waves with velocity $c > 2\omega$ are always smooth, see [26]. Our numerical study indicates that there might not be smooth solitary waves for positive ω and all values of α . If α and thus the dispersion is too small, there might be no such solitary waves. Thus it could be that for $\omega > 0$, there exists a minimal value of α depending on ω and c , $\alpha_s(\omega, c) > 0$, such that only for $\alpha > \alpha_s(\omega, c)$ there exist smooth solitary waves. It also appears that for given α and $\omega > 0$, there exists a minimal velocity $c_s(\omega, \alpha)$ such that there exist smooth solitary waves for $c > c_s$. Since we construct the solitary waves numerically with a Newton iteration, the failure of the iteration only gives an indication that there are no smooth solutions for certain parameters α , c , ω . However, this could also mean that there are no appropriate initial iterates known.

By studying perturbations of the numerically constructed solitary waves, we get

Main conjecture I:

The smooth solitary waves are orbitally stable.

For the CH equation, it was shown in [37], that solutions for smooth initial data u_0 subject to the condition $u_0 - \partial_{xx}u_0 + \omega > 0$ will stay smooth for all times. The precise nature of the singularity that can appear in finite time for initial data not satisfying this non-breaking condition does not appear to be known. Our numerical experiments indicate that for sufficiently small α , initial data satisfying a condition of the form $u_0 + D^\alpha u_0 + \omega > 0$ can develop a cusp in finite time. We have

Main conjecture II:

For sufficiently small $\alpha < \alpha_c(\omega)$, initial data of sufficiently large mass lead to a blow-up of the fCH solution in finite time. The blow-up near a point x_s is a cusp of the form $u \propto \sqrt{|x - x_s|}$.

The precise value of $\alpha_c(\omega)$ and the conditions on the initial data are not known.

This paper is organized as follows: in Section 2 basic facts on the standard CH and the fractional CH equation are gathered and some useful notation is reviewed. In Section 3 the numerical approach is introduced for solitary waves to the fractional CH equation. In Section 4 we investigate numerically the stability properties of solitary waves. The long time behavior of solution to fractional CH equation is studied in the case of initial data from the Schwartz class in Section 5. In Section 6, we study the appearance of rapid modulated oscillations, *dispersive shock waves*, in the vicinity of shocks to the corresponding dispersionless equation. We add some concluding remarks in Section 7.

2. PRELIMINARIES

In this section we collect some basic facts on the standard CH and the fractional CH equation.

We apply the standard definition for a Fourier transform for tempered distributions $u(x)$ denoted by $(\mathcal{F}u)(k)$ with dual variable k and its inverse,

$$(6) \quad \begin{aligned} (\mathcal{F}u)(k) &= \hat{u} = \int_{\mathbb{R}} u(x) e^{-ikx} dx, \quad k \in \mathbb{R}, \\ u(x) &= \frac{1}{2\pi} \int_{\mathbb{R}} (\mathcal{F}u)(k) e^{ikx} dk, \quad x \in \mathbb{R}. \end{aligned}$$

2.1. Conserved Quantities. We give the derivation of the conserved quantities for the equation (1). To this end we consider sufficiently smooth solutions which tend to 0 as $x \rightarrow \mp\infty$. Integrating equation (1) over the real line, we get

$$(7) \quad \frac{d}{dt} \int_{\mathbb{R}} (I + D^\alpha) u dx + \int_{\mathbb{R}} \left(\kappa_1 u + \frac{3}{2} u^2 + \kappa_2 D^\alpha u^2 \right)_x dx + \kappa_2 \int_{\mathbb{R}} u D^\alpha u_x dx = 0.$$

By using Plancherel's theorem, we can rewrite the last integral in equation (7) as

$$\begin{aligned} \int_{\mathbb{R}} u(x, t) D^\alpha u_x(x, t) dx &= \int_{\mathbb{R}} \hat{u}(k, t) |k|^\alpha \overline{ik \hat{u}(k, t)} \frac{dk}{2\pi}, \\ &= \int_{\mathbb{R}} |k|^{\frac{\alpha}{2}} \hat{u} |k|^{\frac{\alpha}{2}} \overline{ik \hat{u}} \frac{dk}{2\pi}, \\ &= \int_{\mathbb{R}} D^{\frac{\alpha}{2}} u D^{\frac{\alpha}{2}} u_x dx, \\ &= \frac{1}{2} \int_{\mathbb{R}} |D^{\frac{\alpha}{2}} u(x, t)|_x^2 dx. \end{aligned}$$

This implies for equation (7)

$$(8) \quad \frac{d}{dt} \int_{\mathbb{R}} (I + D^\alpha) u dx + \int_{\mathbb{R}} \left(\kappa_1 u + \frac{3}{2} u^2 + \kappa_2 D^\alpha u^2 + \frac{\kappa_2}{2} |D^{\frac{\alpha}{2}} u|^2 \right)_x dx = 0,$$

which gives the conserved mass of the fCH equation in the following form

$$(9) \quad I_1 = \int_{\mathbb{R}} (u(x, t) + D^\alpha u(x, t)) dx.$$

For the second conserved quantity, we first multiply both sides of the fCH equation by u and integrate over \mathbb{R} . Then we have

$$\frac{1}{2} \frac{d}{dt} \int_{\mathbb{R}} (u^2 + |D^{\frac{\alpha}{2}} u|^2) dx + \int_{\mathbb{R}} \left(\frac{\kappa_1}{2} u^2 + u^3 + \kappa_2 u^2 D^\alpha u \right)_x dx = 0.$$

Here we have used

$$\int_{\mathbb{R}} u(x, t) D^\alpha (u^2(x, t))_x dx = \int_{\mathbb{R}} D^\alpha u(x, t) (u^2(x, t))_x dx.$$

Finally, the following identity is obtained as formal conserved energy of fCH equation

$$(10) \quad I_2 = \int_{\mathbb{R}} (u^2(x, t) + |D^{\frac{\alpha}{2}} u(x, t)|^2) dx.$$

2.2. Solitary Waves of the CH equation. Solitary waves are localised traveling waves, i.e., solutions of the form $u(x, t) = Q_c(\xi)$, $\xi = x - ct$ with constant propagation speed c and fall-off condition $\lim_{|\xi| \rightarrow \infty} Q_c(\xi) = 0$. This ansatz leads to equation (14) for the fCH equation.

For the integrable CH equation ($\alpha = 2$, $\kappa_1 = 2\omega$, $\kappa_2 = 1/3$), equation (14) can be integrated explicitly leading to

$$(11) \quad (-c(1 - \partial_{xx}) + 2\omega)Q_c + \frac{3}{2}Q_c^2 = Q_c Q_c'' + \frac{1}{2}(Q_c')^2.$$

As discussed in [26], the soliton is given implicitly by

$$(12) \quad Q_c = \frac{(c - 2\omega)\operatorname{sech}^2(\theta)}{\operatorname{sech}^2(\theta) + 2(\omega/c)\tanh^2(\theta)}$$

where

$$(13) \quad x - ct = \sqrt{\frac{4c}{c - 2\omega}}\theta + \ln \frac{\cosh(\theta - \theta_0)}{\cosh(\theta + \theta_0)}$$

with $\theta_0 = \operatorname{arctanh}(\sqrt{1 - (2\omega/c)})$. There is a smooth soliton for $\omega > 0$ and $c > 2\omega$. These solitons are orbitally stable, see [26].

3. SOLITARY WAVES

In this section we numerically construct solitary waves of the fractional CH equation.

3.1. Defining equations. With the traveling wave ansatz $u(x, t) = Q_c(\xi)$, $\xi = x - ct$, equation (1) reduces to the following equation

$$(14) \quad -cQ_c' + \kappa_1 Q_c' + \frac{3}{2}(Q_c^2)' - cD^\alpha Q_c' + \kappa_2 [D^\alpha(Q_c^2)' + Q_c D^\alpha Q_c'] = 0.$$

Here $'$ denotes the derivative with respect to ξ . Integrating we get with the fall-off condition at infinity

$$(15) \quad (-c(1 + D^\alpha) + \kappa_1)Q_c + \frac{3}{2}Q_c^2 + \kappa_2(D^\alpha Q_c^2 + \partial_\xi^{-1}(Q_c D^\alpha Q_c')) = 0.$$

Here the antiderivative is defined via its Fourier symbol, $\mathcal{F}\partial_x^{-1} = 1/(ik)$, i.e., $\partial_x^{-1} = \frac{1}{2}(\int_{-\infty}^x - \int_x^\infty)$.

3.2. Numerical approach. To construct solitary waves numerically, we apply as in [31] a Fourier spectral method. We study equation (15) in the Fourier domain

$$(16) \quad (-c(1 + |k|^\alpha) + \kappa_1)\mathcal{F}Q_c + \frac{3}{2}\mathcal{F}(Q_c^2) + \kappa_2(|k|^\alpha \mathcal{F}(Q_c^2) + \frac{1}{ik}\mathcal{F}(Q_c D^\alpha Q_c')) = 0.$$

The Fourier transform is approximated on a sufficiently large torus ($x \in L[-\pi, \pi]$ with $L \gg 1$) via a discrete Fourier transform (DFT) which is conveniently computed by a fast Fourier transform (FFT). This means we introduce the standard discretisation $x_n = -\pi L + nh$, $n = 1, \dots, N$, $h = 2\pi L/N$ with $N \in \mathbb{N}$ the number of Fourier modes. The dual variable is then given by $k = (-N/2 + 1, \dots, N/2)/L$. In an abuse of notation, we will use the same symbols for the DFT as for the standard Fourier transform.

With the DFT discretisation, equation (16) becomes a system of N nonlinear equations for $\mathcal{F}Q_c$ which is solved with a Newton-Krylov method. This means that

the action of the inverse of the Jacobian in a standard Newton method is computed iteratively with the Krylov subspace method GMRES [38]. Since the convergence of a Newton method is local, the choice of the initial iterate is important. Therefore we apply a tracing technique: the implicit solution for CH ($\alpha = 2$) for some value of the velocity c is taken as the initial iterate for some smaller value of α . The result of this iteration is taken as an initial iterate of an even smaller value of α .

Numerically challenging is the computation of the last term in (16) since there is a division by the dual variable k that can vanish. We apply the same approach as in [29], the limiting value for $k = 0$ is computed via de l'Hospital's rule, $\lim_{k \rightarrow 0} \hat{f}(k)/k = \hat{f}'(0)$ if $\hat{f}'(k)$ is bounded for $k = 0$. The derivative for $k = 0$ is computed in standard way via the sum of the inverse Fourier transform f of the function \hat{f} times x sampled at the collocation points in x , see [29], i.e., $\hat{f}'(0) \approx \sum_{n=1}^N x_n f_n$.

3.3. Examples. To study concrete examples, we work with $L = 100$ and $N = 2^{16}$ as in [31] for fractional Korteweg-de Vries (fKdV) equations. We consider the case $\kappa_2 = 1/3$, $\kappa_1 = 2\omega$ being integrable for $\alpha = 2$. We choose $\omega = 3/5$ as in [16]. We show solitary waves for $c = 2$ for several values of α in Fig. 1. It can be seen that the smaller α and thus the dispersion, the more the solitary wave is peaked and the slower the decay towards infinity. We were not able to numerically find a solution for even smaller values of α since the iteration did not converge to a smooth solution. The behavior of the DFT coefficients in the iteration indicates that it converges to a peakon or cuspon. This does not mean that there are no smooth solitary waves for smaller values of α for this velocity, we just could not find them with a Newton iteration. But this could indicate that there might be for a given c a lower limit $\alpha_s(\omega, c)$ for α below which there are no smooth solitons; we recall that there are smooth solitons for CH for all positive ω with $c > 2\omega$. Note, however, that it is difficult to identify such a limit with an iterative method since the failure of the latter to converge does not mean that there is no such solution. It can be that the initial iterate was just not sufficiently close.

The amplitude of the solitary waves increases with the velocity c . We show this behavior on the left of Fig. 2 for $\alpha = 1.5$, $\omega = 0.6$ and several values of c . For CH solitons one has $c > 2\omega$. There is clearly also a lower bound on the velocity for smooth solitons larger than the $c > 2\omega$ limit for CH, but it is not clear whether it is larger than the value for CH. Once more such a value cannot be determined with an iterative approach. If one fixes c and α , there does not appear to be an obvious dependence between ω and the amplitude as in the case of CH as can be seen on the right of Fig. 2.

Note that the precise fall-off of the solitary waves for $|x| \rightarrow \infty$ appears to be unknown, it should be the same $|x|^{-(1+\alpha)}$ rate of solitary waves of the fractional Korteweg-de Vries and nonlinear Schrödinger equation, see [22]. But it is numerically difficult to determine the exact fall-off rate on the real line via an approximation on a torus.

4. STABILITY OF THE SOLITARY WAVES

In this section we study the stability of the solitary waves under small perturbations. For various perturbations, the solitary waves appear to be stable providing numerical evidence to the first part of the Main Conjecture.

4.1. Numerical approach. To study the time evolution of solutions to the fractional CH equation (1), we use the same spatial discretisation as in the previous section, i.e., a standard FFT approach. The time integration is done with the well

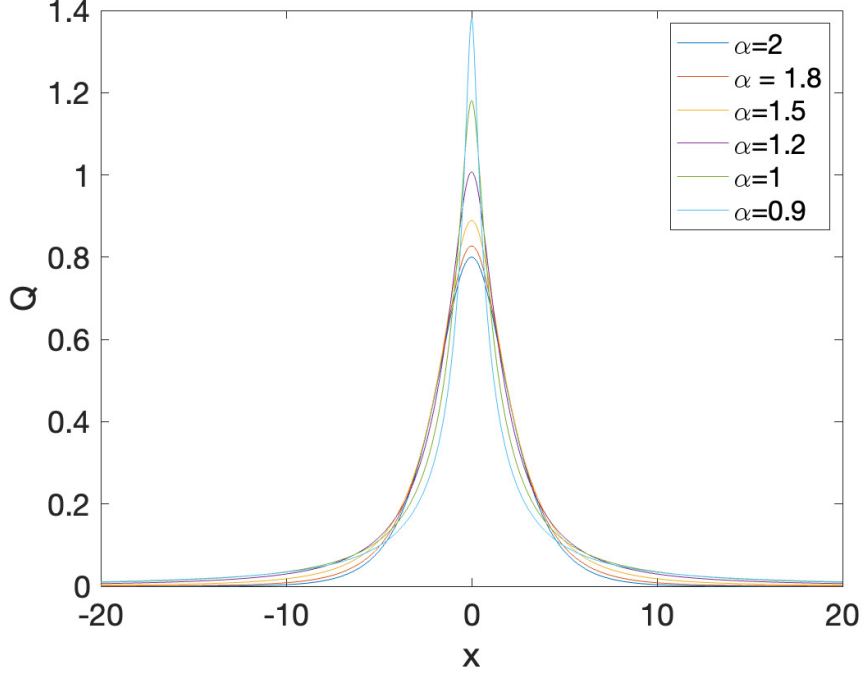


FIGURE 1. Solitary waves (15) for $c = 2$, $\kappa_1 = 1.2$, $\kappa_2 = 1/3$ for several values of α .

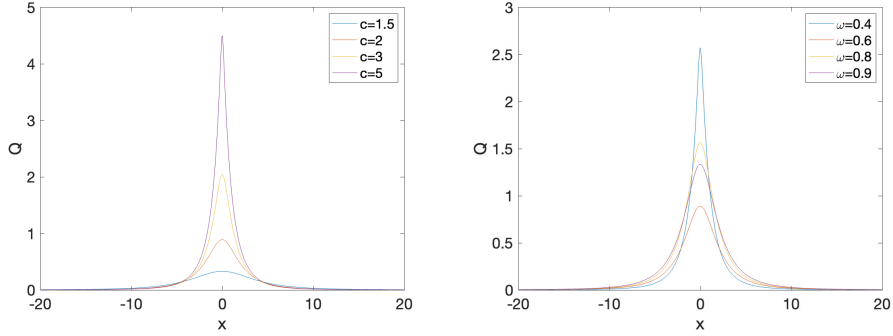


FIGURE 2. Solitary waves (15) for $\kappa_2 = 1/3$ and $\alpha = 1.5$, on the left for $\omega = 0.6$ and several values of c , on the right for $c = 2$ and several values of ω .

known explicit Runge-Kutta method of 4th order. The accuracy of the time integration is controlled via the conserved energy (10) which will numerically depend on time due to unavoidable numerical errors. As discussed in [28], this numerically computed energy will overestimate the numerical error by 2-3 orders of magnitude. Thus we will always track in the following the relative energy and the DFT coefficients to control the numerical resolution.

As a test we propagate the solitary wave for $c = 2$, $\alpha = 1.5$, $\omega = 3/5$ and use $N_t = 10^4$ time steps for $t \in [0, 1]$. The relative energy is conserved during the whole computation to the order of 10^{-15} . The DFT coefficients decrease to machine precision (here 10^{-16}) which means that the solution is well resolved both

in space and in time. The difference between the solitary wave travelling with velocity $c = 2$ and the numerically computed solution for $t = 1$ is of the order 10^{-15} . This shows that the code is able to propagate solitary waves with machine precision as indicated by the numerical conservation of the energy and the DFT coefficients. In addition it shows that the solitary waves numerically constructed in the previous section are indeed solutions to equation (15) with a similar accuracy.

4.2. Perturbed solitary waves. We consider perturbations of the solitary waves in the form of perturbed initial data,

$$(17) \quad u(x, 0) = Q_c + Ae^{-x^2},$$

where A is a small real constant. In all examples below, the DFT coefficients always decrease to machine precision, and the relative energy is conserved to better than 10^{-6} .

First we consider the case $\alpha = 1.5$ for Q_2 and $A = \pm 0.08$. This corresponds to a perturbation of the order of 10%. This is not a small perturbation, but in order to see numerical effects of a perturbation in finite time, it is convenient to consider perturbations that are of the order of a few percent. We use $N_t = 10^4$ time steps for $t \leq 40$. In Fig. 3 we show on the left the solution for $t = 40$. The solution appears to be a solitary wave with some radiation propagating towards $-\infty$. This is confirmed by the L^∞ norm of the solution on the right of the same figure. After some time the L^∞ norm appears to reach an asymptotic value corresponding to a slightly faster soliton. This is due to the fact that we considered a perturbation of almost 10%. The final state is thus a solitary wave with larger mass, the solitary wave appears to be stable.

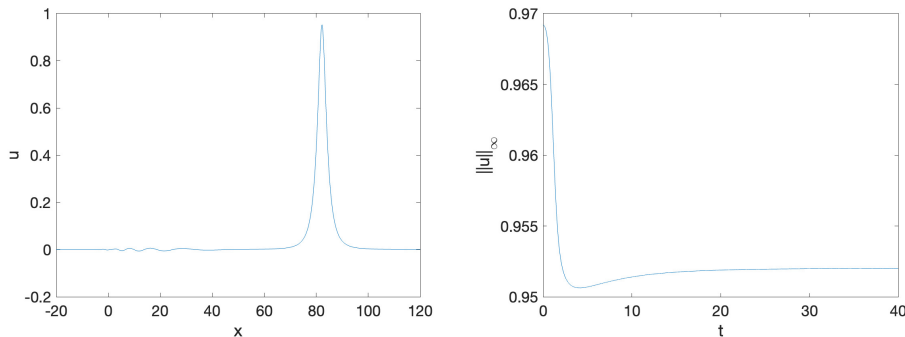


FIGURE 3. Solution to the fractional CH equation for initial data of the form (17) with $A = 0.08$ for $\alpha = 1.5$ and $c = 2$: on the left the solution for $t = 40$, on the right the L^∞ norm of the solution in dependence of time.

We obtain a similar result if we consider a perturbation of the solitary wave with slightly smaller mass than the unperturbed solitary wave. In Fig. 4, we choose initial data of the form (17) with $A = -0.08$ with the same parameters as in Fig. 3. The solution at the final time $t = 40$ appears to be again a solitary wave plus radiation. This is confirmed by the L^∞ norm on the right of the same figure. The final state of the solution appears to be a solitary wave with a slightly smaller mass and velocity than Q_2 . The solitary wave seems to be again stable even against comparatively large perturbations.

It is an interesting question whether a similar behavior can be observed for smaller values of α , i.e., for a fractional CH equation with less dispersion. We

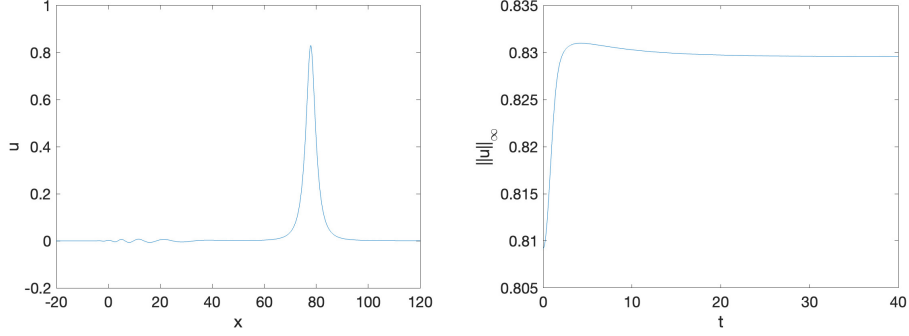


FIGURE 4. Solution to the fractional CH equation for initial data of the form (17) with $A = -0.08$ for $\alpha = 1.5$ and $c = 2$: on the left the solution for $t = 40$, on the right the L^∞ norm of the solution in dependence of time.

consider the case $\alpha = 0.9$ for which we could construct solitary waves with $c = 2$. Here we consider smaller perturbations of the order of 1% for larger times than before. We apply $N_t = 2 * 10^4$ time steps for $t \leq 100$ to initial data of the form (17). In Fig. 5 we show on the left the L^∞ norm of the solution for $A = 0.01$ and on the right for $A = -0.01$. In both cases the final state of the solution appears to be a solitary wave plus radiation. The small oscillations in the L^∞ norm are due to the fact that we are working on a torus where the radiation can reenter the computational domain on the other side and that we determine the maximum of the solution on grid points.

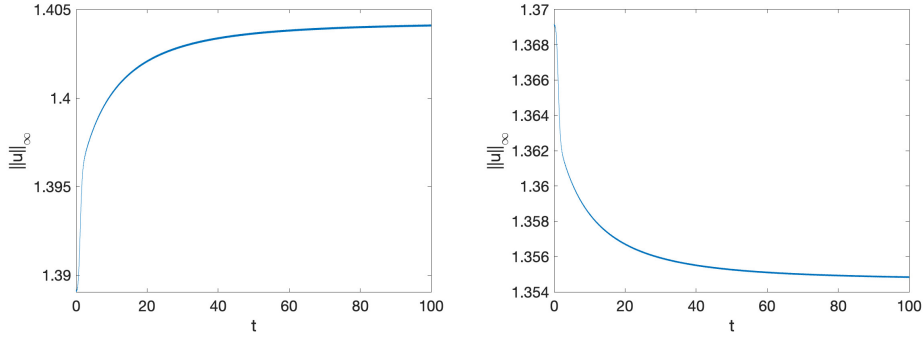


FIGURE 5. L^∞ norm of the solution to the fractional CH equation for initial data of the form (17) for $\alpha = 0.9$ and $c = 2$: on the left for $A = 0.01$, on the right for $A = -0.01$.

The picture is very similar for different types of perturbations. We consider the solution for initial data of the form $u(x, 0) = \lambda Q_2(x)$ for $\alpha = 0.9$ and real λ close to 1. In Fig. 6, the L^∞ norms of the solution in dependence of time is shown, on the left for $\lambda = 0.99$, on the right for $\lambda = 1.01$. In both cases the final state appears to be a solitary wave of slightly different mass.

5. LOCALIZED INITIAL DATA

In this section we study the long time behavior of initial data from the Schwartz class of smooth rapidly decreasing functions. We are interested whether solitary

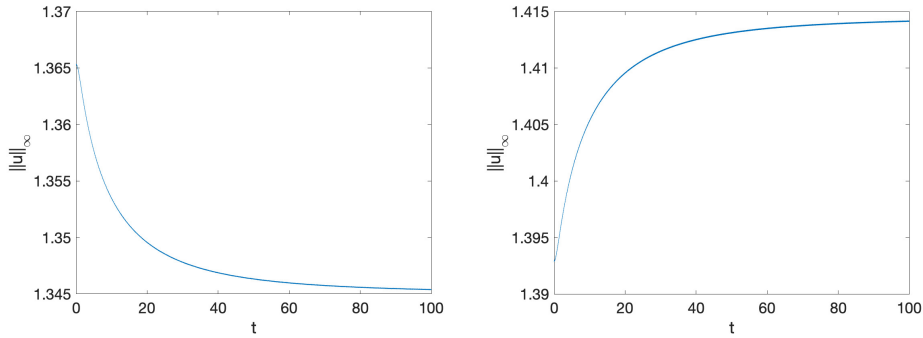


FIGURE 6. L^∞ norm of the solution to the fractional CH equation for initial data of the form $u(x, 0) = \lambda Q_2(x)$ for $\alpha = 0.9$ and $c = 2$: on the left for $\lambda = 0.99$, on the right for $\lambda = 1.01$.

waves appear in the solution asymptotically as expected from the *soliton resolution conjecture*, or whether there is a *blow-up*, a loss of regularity of the solution in finite time.

Concretely we will study Gaussian initial data,

$$(18) \quad u(x, 0) = A \exp(-x^2),$$

where $A > 0$ is constant. We will use $N_t = 10^4$ time steps and $N = 2^{14}$ Fourier modes for $x \in 3[-\pi, \pi]$. We first study the case $\alpha = 1.5$. Small initial data will be simply radiated towards infinity. But if we take initial data of the form (18) with $A = 1$, we get the solution shown in Fig. 7. The initial hump breaks up into several humps. One of them, possibly three, appear to be solitary waves. It seems that the solution indeed decomposes into solitary waves and radiation. The precise number of solitary waves appearing for large times is unknown.

The interpretation of the largest hump as a solitary wave is confirmed by the L^∞ norm of the solution shown in Fig. 8 on the right. It seems to reach a constant asymptotic value as expected for a solitary wave. Since the solitary waves for the fractional CH equation do not have a simple scaling with the velocity c as the fKdV solitary wave, a fit of the hump to the solitary waves is not obvious. The solution for $t = 20$ is shown on the left of Fig. 8.

For smaller values of α , the picture can change. If we take $\alpha = 0.9$ and initial data of the form (18) with $A = 0.5$, the initial hump will be radiated away. The solution for $t = 40$ is shown on the left of Fig. 9. The L^∞ norm of the solution on the right of the same figure appears to decrease monotonically with time.

However for initial data of the form (18) of larger mass, i.e., larger values of A , we do not find solitary waves in the long time behavior of the solution. Instead for $A = 1$, a cusp appears to form in finite time, for $t \sim 1.7667$ in this case. The solution at this time can be seen in Fig. 10 on the left.

It is not only the figure that indicates a cusp formation, this is also confirmed by the Fourier coefficients (more precisely the DFT of u) on the right of the same figure. The algebraic decay of these coefficients with the index $|k|$ indicates that a singularity of the analytic continuation of the function u to the complex plane will hit at the critical time the real axis. It is well known that an essential singularity in the complex plane of the form $u \sim (z - z_j)^{\mu_j}$, $\mu_j \notin \mathbb{Z}$, with $z_j = \alpha_j - i\delta_j$ in the lower half plane ($\delta_j \geq 0$) implies for $k \rightarrow \infty$ the following asymptotic behavior of

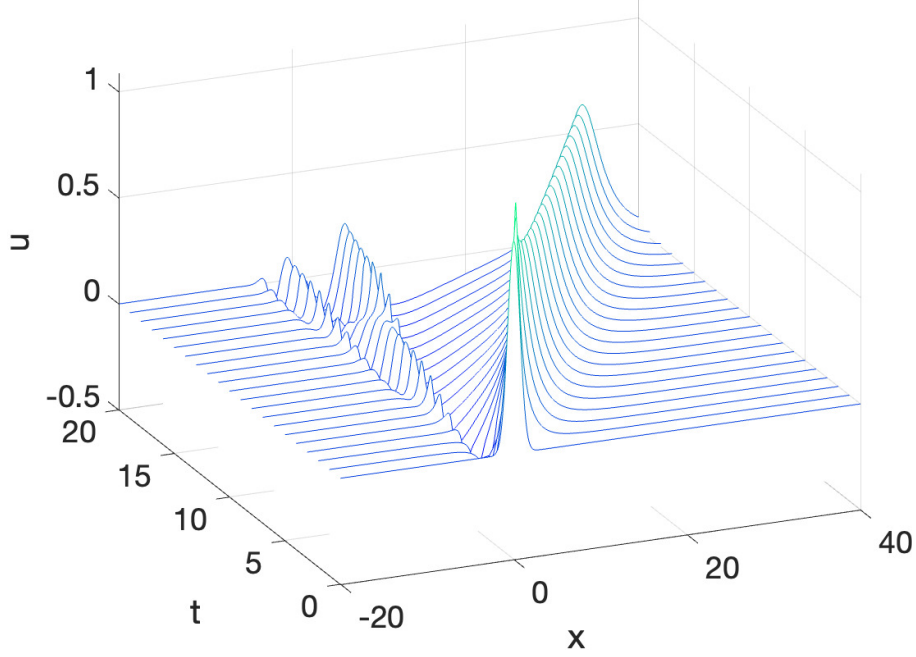


FIGURE 7. Solution to the fractional CH equation with $\alpha = 1.5$ for initial data $u(x,0) = \exp(-x^2)$.

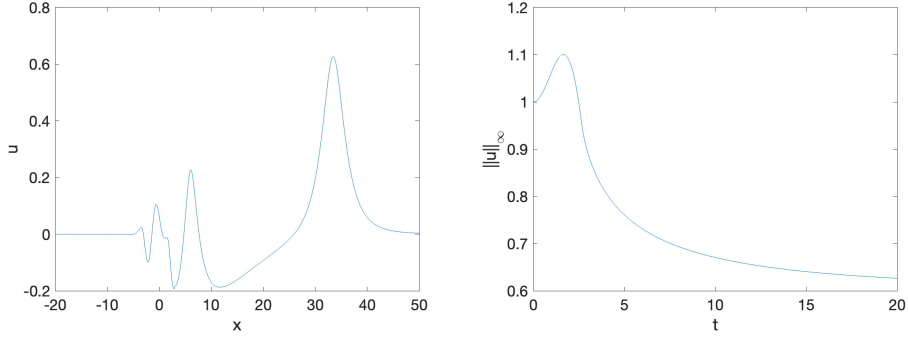


FIGURE 8. Solution to the fractional CH equation with $\alpha = 1.5$ for initial data $u(x,0) = \exp(-x^2)$, on the right the L^∞ norm, on the left the solution for $t = 20$.

the Fourier coefficients (see e.g. [6]),

$$(19) \quad \hat{u} \sim \sqrt{2\pi} \mu_j^{\mu_j + \frac{1}{2}} e^{-\mu_j} \frac{(-i)^{\mu_j + 1}}{k^{\mu_j + 1}} e^{-ik\alpha_j - k\delta_j}.$$

For a single such singularity with positive δ_j , the modulus of the Fourier coefficients decreases exponentially for large k until $\delta_j = 0$, when the modulus of the Fourier coefficients has an algebraic dependence on k . As first shown in [39], one can use (19) to numerically characterize the singularity as discussed in detail in [30] (the DFT coefficients have a similar behavior as the Fourier transform). Essentially a least square method is applied to $\ln |\hat{u}|$ to fit the parameters for $k > 100$. The reader is referred to [30] for details. For the case shown in Fig. 10, we find $\mu = 0.5007$. This

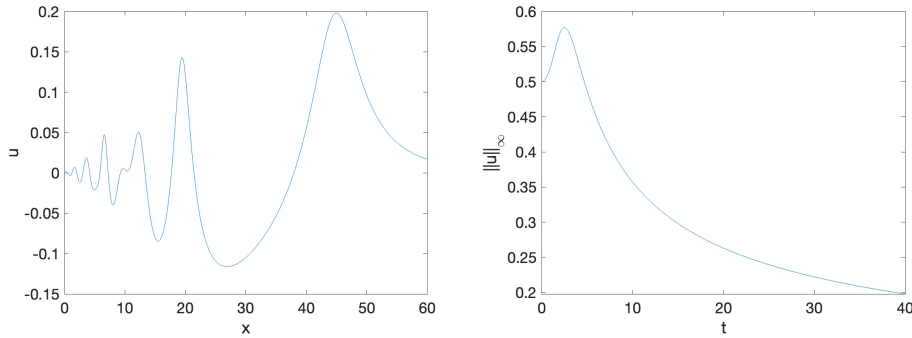


FIGURE 9. Solution to the fractional CH equation with $\alpha = 0.9$ for initial data $u(x, 0) = 0.5 \exp(-x^2)$, on the left the solution for $t = 40$, on the right the L^∞ norm.

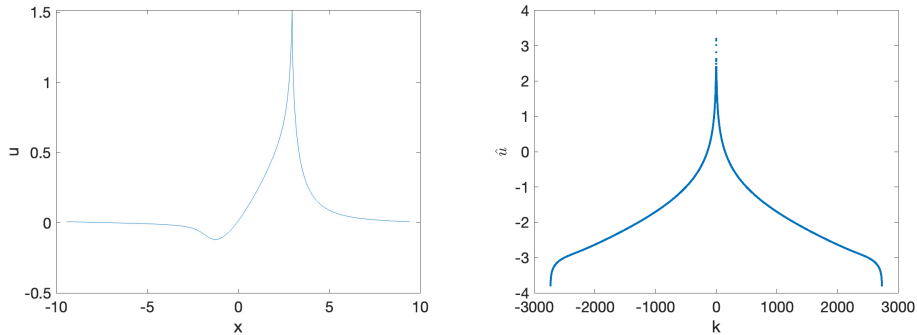


FIGURE 10. Solution to the fractional CH equation with $\alpha = 0.9$ for initial data $u(x, 0) = \exp(-x^2)$, on the left the solution for $t = 1.7667$, on the right the DFT coefficients for this solution.

means that a square root type singularity is observed in this case which provides numerical evidence of the second part of the main conjecture in the introduction. Since global existence in time does not appear to hold for solutions to initial data of sufficiently large mass, no solitary waves are observed in this case.

Note that this is in apparent contradiction to the stability of the solitary waves observed numerically in the previous section. However, it has to be remembered that the solitary waves have a slow algebraic fall-off towards infinity whereas we consider exponentially decaying data in this section. For L^2 -critical generalized Korteweg-de Vries equations, a blow-up in finite time is only observed if the initial data are sufficiently rapidly decreasing, see [36] and references therein. The situation appears to be similar for fCH solutions for sufficiently small α .

6. DISPERSIVE SHOCK WAVES

In this section we study the appearance of dispersive shock waves (DSWs) in fCH solutions. A convenient way to study the formation of zones of rapid oscillations in the solutions of dispersive PDEs is to consider the solution for large times on large scales. This can be done by introducing a small parameter $\epsilon \ll 1$ and rescale t, x according to $t \mapsto t/\epsilon, x \mapsto x/\epsilon$. This leads for equation (1) to

$$(20) \quad u_t + \kappa_1 u_x + 3uu_x + \epsilon^\alpha D^\alpha u_t = -\kappa_2 \epsilon^\alpha [2D^\alpha(uu_x) + uD^\alpha u_x],$$

where we have kept the same notation as for the case $\epsilon = 1$. Thus equation (20) is simply equation (1) with D^α replaced by $\epsilon^\alpha D^\alpha$. In the formal limit $\epsilon \rightarrow 0$, equation (20) reduces to the Hopf equation

$$(21) \quad u_t + \kappa_1 u_x + 3uu_x = 0,$$

where the term linear in u_x can be absorbed by a Galilei transformation. The Hopf equation is known to develop a gradient catastrophe for hump-like initial data in finite time. Dispersive regularisations of this equation as (20) are expected to lead to solutions with zones of rapid oscillations in the vicinity of the shocks of the Hopf solution for the same initial data.

In [23], we have studied numerically the onset of oscillations in solutions of the CH equation. It was conjectured that a special solution to the second equation in the Painlevé I hierarchy, see for instance [24], provides an asymptotic description of the break-up of CH solutions in this case. For larger times the oscillatory zone was studied in [1]. A conjecture to describe the leading edge of the oscillatory zone in terms of a Painlevé transcendent was given.

We will study below similar examples as in [23, 1] for fCH, initial data of the form $u(x, 0) = \text{sech}^2 x$ for several values of ϵ . In Fig. 11, we show the fCH solution for $\alpha = 1.5$ and $\epsilon = 10^{-2}$ for several values of t . We use $N = 2^{14}$ Fourier modes and $N_t = 10$ time steps for $t \leq 1$. A first oscillation forms for $t \sim 0.4$ (the critical time for the Hopf solution is $t_c \sim 0.433$), then a well defined zone of oscillations appears also called the Whitham zone.

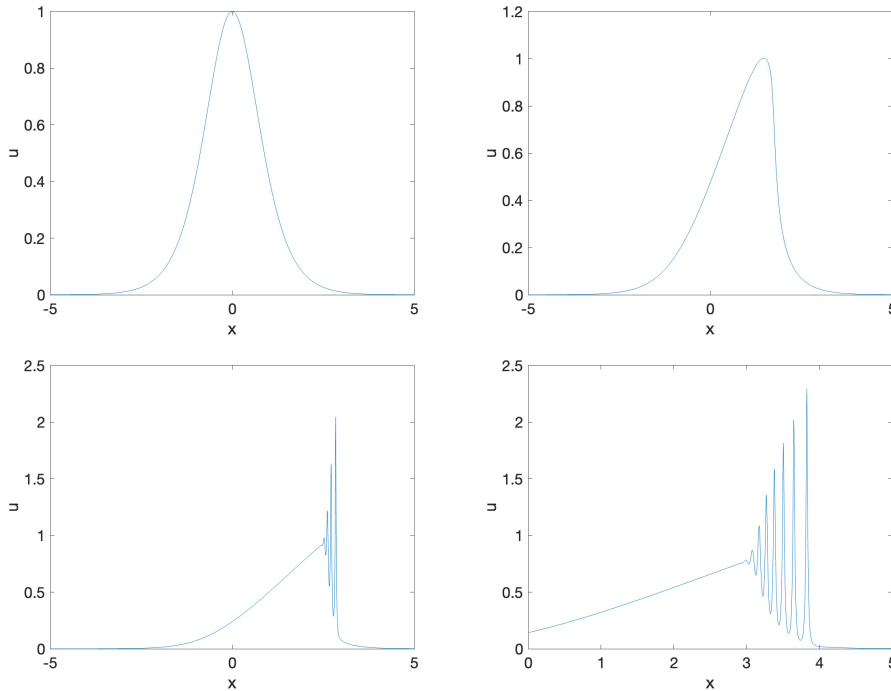


FIGURE 11. Solution to the fractional CH equation (20) with $\alpha = 1.5$, $\omega = 0.6$ and $\epsilon = 10^{-2}$ for initial data $u(x, 0) = \text{sech}^2 x$ for several values of time (on the top for $t = 0$, $t = 0.35$, in the bottom for $t = 0.7$, $t = 1$).

The Whitham zone becomes more defined and more oscillatory the smaller ϵ is. Thus there is no strong limit $\epsilon \rightarrow 0$ for DSWs. Note that DSWs in CH solutions

are numerically more demanding than the corresponding KdV solutions for which special integrators exist, see for instance [28]. For CH time integration is more problematic since the dispersive terms are nonlinear in contrast to KdV. The reduced dispersion in CH compared to KdV because of the nonlocality $((1 - \partial_{xx})u_t$ leads to less oscillations in CH than in similar KdV situations, but to stronger gradients). This is amplified in fCH solutions since the dispersion is smaller than in CH. To treat the case $\epsilon = 10^{-3}$ for the situation shown in Fig. 11, we apply $N = 2^{18}$ Fourier modes and $N_t = 10^5$ time steps. We show the fCH solution for three values of ϵ in Fig. 12 for the same initial data at the same time.

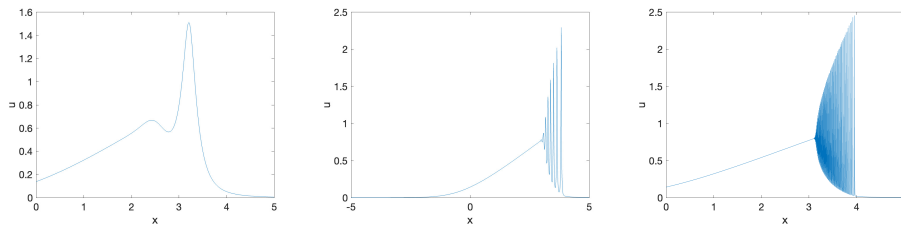


FIGURE 12. Solution to the fractional CH equation (20) with $\alpha = 1.5$, $\omega = 0.6$ for initial data $u(x, 0) = \text{sech}^2 x$ for $t = 1$ for $\epsilon = 10^{-1}$, $\epsilon = 10^{-2}$, $\epsilon = 10^{-3}$ from left to right.

For smaller α , the dispersion is even weaker. For the same initial data as in Fig. 12, we get for $\alpha = 0.9$ and $\epsilon = 10^{-1}$ again a DSW as can be seen in Fig. 13. As expected the smaller dispersion than in Fig. 12 leads to less oscillatory behavior.

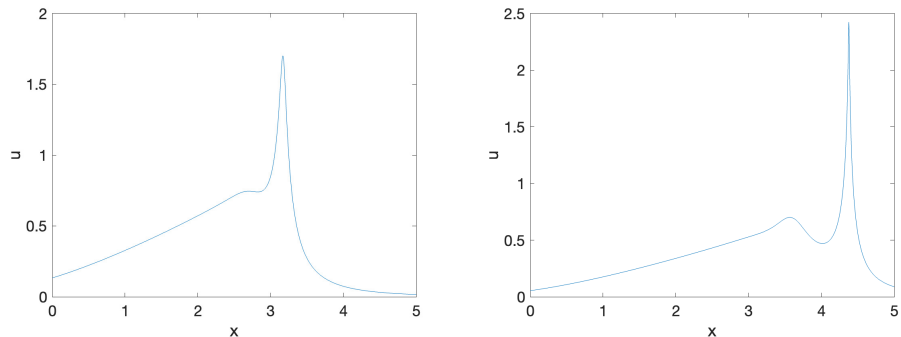


FIGURE 13. Solution to the fractional CH equation (20) with $\alpha = 0.9$, $\omega = 0.6$ and $\epsilon = 10^{-1}$ for initial data $u(x, 0) = \text{sech}^2 x$ for $t = 1.005$ on the left and $t = 1.5$ on the right.

However the situation is different for smaller ϵ than in Fig. 13, $\epsilon = 10^{-2}$, as can be seen in Fig. 14. We use $N = 2^{15}$ Fourier modes and $N_t = 10^4$ time steps for $t \leq 0.7$. There is once more a DSW forming, but the first peak appears to develop in finite time into a cusp, see the left of Fig. 14. It is not surprising that a smaller ϵ leads to a cusp formation that was already observed in the previous section for initial data of sufficient mass in this case. Since the formal rescaling of x and t with ϵ leads also to a rescaling of the mass, the same initial data will have more mass in the original setting (1) the smaller ϵ . The cusp formation is confirmed by the DFT coefficients on the right of the figure which gives more numerical evidence to the second part of the Main Conjecture. A fitting of the coefficients to (19) indicates an exponent $\mu \sim 0.68$. This is slightly larger than the factor $1/2$ found

in the previous section, but the accuracy in identifying the factor μ is always less than for the exponent δ in (19), in particular here where the DSW already leads to a slower decay of the DFT coefficients with the index k . Thus there is strong evidence for cusp formation, but the exact character of the singularity needs to be justified analytically.

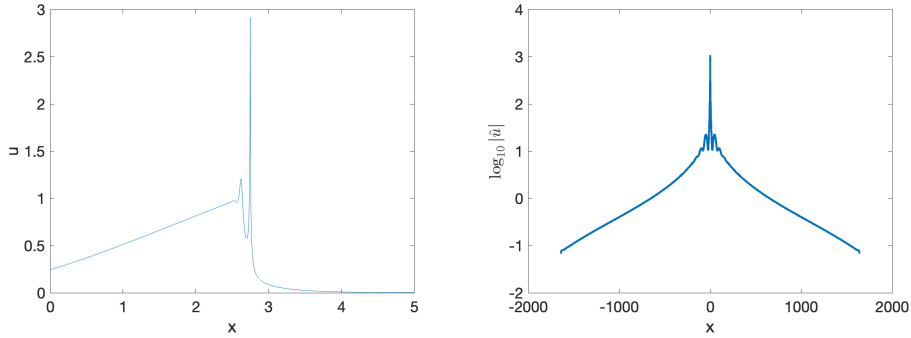


FIGURE 14. Solution to the fractional CH equation (20) with $\alpha = 0.9$, $\omega = 0.6$ and $\epsilon = 10^{-2}$ for initial data $u(x, 0) = \text{sech}^2 x$ for $t = 0.6819$ on the left and the DFT coefficients on the right.

7. OUTLOOK

In this paper, we have started a numerical study of the fractional CH equation. Solitary waves have been numerically constructed, and indications have been found that there could be a minimal value of α for given velocity c and positive parameter ω below which there are no smooth solitary waves. It was shown that the numerically constructed smooth solitary waves are stable. A study of initial data from the Schwartz class of smooth rapidly decreasing functions led for initial data of small mass to scattering. For higher mass and sufficiently large α , solitary waves seem to be observed for large times in accordance with the soliton resolution conjecture. However, for smaller values of α , cusps can appear in finite time for such initial data. We also studied the formation of dispersive shock waves.

An interesting question raised by this study is to identify the parameter space α , ω and c for which smooth solitary waves exist. The fall-off behavior of these solutions should be proven. The orbital stability of these solitary waves is a question to be addressed also analytically. Of particular interest is the question of a blow-up already in the CH equation, and even more so in fCH, for which initial data a globally smooth solution in time can be expected, and for which data a blow-up in finite time is to be expected. The type of blow-up appears to be a gradient catastrophe, but this needs to be confirmed analytically.

The formation of DSWs was shown numerically. In [23, 1], the onset of the oscillations as well as the boundary of the Whitham zone was conjectured to be asymptotically given by certain Painlevé transcendents. It is an interesting question whether there are fractional ODEs that play a role in this context for the fCH equation. It will be the subject of further research to address such questions.

REFERENCES

- [1] S. Abenda, T. Grava and C. Klein, Numerical Solution of the Small Dispersion Limit of the Camassa-Holm and Whitham Equations and Multiscale Expansions, *SIAM J. Appl. Math.* 70(8) (2010) 2797-2821.

- [2] M.S. Alber, R. Camassa, D.D. Holm, J.E. Marsden, The geometry of peaked solitons and billiard solutions of a class of integrable PDE's, *Lett. Math. Phys.* 32 (1994) 137–151.
- [3] R. Artebrant, H.J. Schroll, Numerical simulation of Camassa-Holm peakons by adaptive upwinding, *Appl. Numer. Math.* 56(5) (2006) 695–711.
- [4] R. Camassa, D. Holm, An integrable shallow water equation with peaked solitons, *Phys. Rev. Lett.* (1993) 1661–1664.
- [5] R. Camassa, J. Huang, L. Lee, On a completely integrable numerical scheme for a nonlinear shallow-water wave equation, *J. Non. Math. Phys.* 12(sup1) (2005) 146–162.
- [6] G. Carrier, M.K.C. Pearson, *Functions of a Complex Variable, Theory and Technique*, SIAM, 2005.
- [7] G.M. Coclite, K.H. Karlsen, N.H. Risebro, A Convergent Finite Difference Scheme for the Camassa–Holm Equation with General H^1 Initial Data, *SIAM J. Num. Anal.* 46(3) (2008) 1554–1579.
- [8] G.M. Coclite, K.H. Karlsen, N.H. Risebro, An explicit finite difference scheme for the Camassa-Holm equation, (2008) 681–732.
- [9] A. Constantin, J. Escher, Wave breaking for nonlinear nonlocal shallow water equations, *Acta Math.* 181(2), (1998) 229–243.
- [10] A. Constantin, B. Kolev, On the geometric approach to the motion of inertial mechanical systems, *J. Phys. A Math.* 35(32) (2002) R51.
- [11] A. Constantin, B. Kolev, Geodesic flow on the diffeomorphism group of the circles, *Comment. Math. Helvetici* 78 (2003) 787–804.
- [12] A. Constantin, W. Strauss, Stability of peakons, *Commun. Pure Appl. Math.* (2000) 603–610.
- [13] A. Constantin, W. Strauss, Stability of Camassa-Holm solitons, *J. Nonlinear Sci.* (2002) 412–422.
- [14] H.R. Dullin, A.G. Gottwald, D.D. Darryl, An integrable shallow water equation with linear and nonlinear dispersion, *Phys. Review Lett.* 87(19) (2001) 194501.
- [15] N. Duruk Mutlubas, On the Cauchy problem for the fractional Camassa–Holm equation, *Mon. Hefte. Math.* 190(4) (2019) 755–768.
- [16] H.A. Erbay, S. Erbay, A. Erkip, Derivation of the Camassa–Holm equations for elastic waves, *Phys. Lett. A* 379(12–13) (2015) 956–961.
- [17] L. Fan, H. Gao, The Cauchy problem for generalized fractional Camassa–Holm equation in Besov space, *Mon. Hefte. Math.* 195 (2021) 451–475.
- [18] L. Fan, H. Gao, J. Wang, W. Yan, The Cauchy problem for fractional Camassa-Holm equation in Besov space, *Nonlinear Anal. Real World Appl.* 61 (2021) 103348.
- [19] B.-F. Feng, K. Maruno, Y. Ohta, A self-adaptive moving mesh method for the Camassa-Holm equation, *J. Comput. Appl. Math.* 235(1) (2010) 229–243.
- [20] M. Fisher, J. Schiff, The Camassa Holm equation: conserved quantities and the initial value problem, *Phys. Lett. A* 259(5) (1999) 371–376.
- [21] A. Fokas, B. Fuchssteiner, Symplectic structures, their Bäcklund transformations and hereditary symmetries, *Physica D* 4 (1981) 44–66.
- [22] R.L. Frank, E. Lenzmann, On the uniqueness and non degeneracy of ground states of $(-\Delta)^s Q + Q - Q^{\alpha+1} = 0$ in \mathbb{R} , *Acta Math.* (<http://arxiv.org/abs/1009.4042>).
- [23] T. Grava, C. Klein, Numerical study of a multiscale expansion of KdV and Camassa-Holm equation, in *Integrable Systems and Random Matrices*, ed. by J. Baik, T. Kriecherbauer, L.-C. Li, K.D.T-R. McLaughlin, C. Tomei, *Contemp. Math.* 458 (2008) 81–99.
- [24] T. Grava, A. Kapaev, C. Klein On the tritronquée solutions of P_I^2 , *Constr. Approx.* 41 (2015) 425–466.
- [25] H. Holden, X. Raynaud, Convergence of a finite difference scheme for the Camassa–Holm equation, *SIAM J. Num. Anal.* 44(4) (2006) 1655–1680.
- [26] R. Johnson, On solutions of the Camassa–Holm equation, *Proc. Royal Soc. A* 456(2035) (2003) 1687–1708.
- [27] H. Kalisch, J. Lenells, Numerical study of traveling-wave solutions for the Camassa–Holm equation, *Chaos Solit. Fractals* 25(2) (2005) 287–298.
- [28] C. Klein, Fourth order time-stepping for low dispersion Korteweg-de Vries and nonlinear Schrödinger equation, *Electron. Trans. Numer. Anal.* 29 (2008) 116–135.
- [29] C. Klein, K. McLaughlin, N. Stoilov, High precision numerical approach for Davey-Stewartson II type equations for Schwartz class initial data, *Proc. Royal Soc. A* 476(2239) (2020) 20190864.
- [30] C. Klein, K. Roidot, Numerical study of shock formation in the dispersionless Kadomtsev-Petviashvili equation and dispersive regularizations, *Physica D* 265 (2013) 1–25.
- [31] C. Klein, J.-C.Saut, A numerical approach to blow-up issues for dispersive perturbations of Burgers' equation, *Physica D* 295 (2015) 46–65.

- [32] S. Kouranbaeva, The Camassa–Holm equation as a geodesic flow on the diffeomorphism group, *J. Math. Phys.* 40(2) (1999) 857–868.
- [33] J. Lenells, Stability of periodic peakons, *Int. Math. Res. Notices*, 10 (2004) 485–499.
- [34] J. Lenells, A variational approach to the stability of periodic peakons, *J. Math. Phys.* 11(2) (2004) 151–163.
- [35] J. Lenells, Traveling wave solutions of the Camassa–Holm equation, *J. Differ. Equ.* 217(2) (2005) 393–430.
- [36] Y. Martel, F. Merle, P. Raphaél, Blow up for the critical gKdV equation I: dynamics near the soliton. *Acta Math.* 212 (2014) 59–140.
- [37] H. P. McKean, Breakdown of the Camassa–Holm equation, *Comm. Pure Appl. Math.* 57 (2004) 416–418.
- [38] Y. Saad, M. Schultz, GMRES: A generalized minimal residual algorithm for solving nonsymmetric linear systems, *SIAM J. Sci. Stat. Comput.* 7(3) (1986) 856–869.
- [39] C. Sulem, P. Sulem, H. Frisch, Tracing complex singularities with spectral methods, *J. Comp. Phys.* 50 (1983) 138–161.
- [40] Y. Xu, C-W. Shu, A local discontinuous Galerkin method for the Camassa–Holm equation, *SIAM J. Numer. Anal.* 46(4) (2008) 1998–2021.

INSTITUT DE MATHÉMATIQUES DE BOURGOGNE, UMR 5584, INSTITUT UNIVERSITAIRE DE FRANCE,
UNIVERSITÉ DE BOURGOGNE-FRANCHE-COMTÉ, 9 AVENUE ALAIN SAVARY, 21078 DIJON CEDEX,
FRANCE, E-MAIL CHRISTIAN.KLEIN@U-BOURGOGNE.FR

INSTITUT DE MATHÉMATIQUES DE BOURGOGNE, UMR 5584, UNIVERSITÉ DE BOURGOGNE-
FRANCHE-COMTÉ, 9 AVENUE ALAIN SAVARY, 21078 DIJON CEDEX, FRANCE, E-MAIL TOPKARCI@ITU.EDU.TR